LASER INTERFEROMETER GRAVITATIONAL WAVE OBSERVATORY

LIGO Laboratory / LIGO Scientific Collaboration

LIGO-T1200472-v1 *LIGO* October 4, 2012

BS02 reflection and transmission maps' profile and effects

Hiro Yamamoto

Distribution of this document:
LIGO Science Collaboration

This is an internal working note
of the LIGO Project.

California Institute of Technology
LIGO Project – MS 100-36
1200 E. California Blvd.
Pasadena, CA 91125
Phone (626) 395-2129
Fax (626) 304-9834
E-mail: info@ligo.caltech.edu

Massachusetts Institute of Technology
LIGO Project – NW22-295
185 Albany St
Cambridge, MA 02139
Phone (617) 253-4824
Fax (617) 253-7014
E-mail: info@ligo.mit.edu

LIGO Hanford Observatory
P.O. Box 1970
Mail Stop S9-02
Richland WA 99352
Phone 509-372-8106
Fax 509-372-8137

LIGO Livingston Observatory
P.O. Box 940
Livingston, LA 70754
Phone 225-686-3100
Fax 225-686-7189

http://www.ligo.caltech.edu/

1. Introduction

The reflection and transmission maps of BS02 were measured at LIGO Lab, E1000788. Profiles of those maps and effects on the beams interacting with BS02 are analyzed in this note. All maps have large noise components with high spatial frequency, which are introduced by the measurement process. The reflection map on the AR side, i.e., reflection between the signal recycling cavity (SRC) and the x-arm, is the worst among the four maps, due to high figure terms (low spatial frequency component). This may induce 1% of higher order mode power by this reflection, or ~10W in the dark side of the BS at the full power operation.

2. BS geometry

Fig.1 shows the geometry of a BS mirror. P, S, X and Y are the directions pointing to power recycling cavity (PRC), signal recycling cavity (SRC), X and Y arm respectively. When describing a field, a right handed coordinate system is used, where z is pointing toward the beam propagation direction, y upward perpendicular to the IFO plane, and x to form a right handed system.

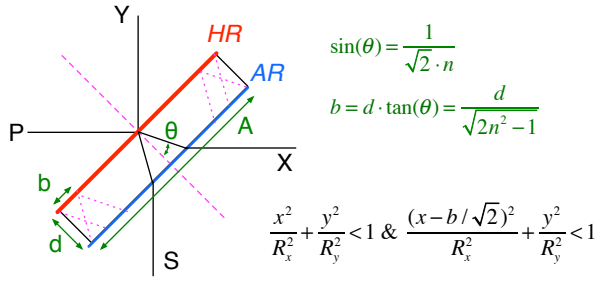

Figure 1 BS geometry

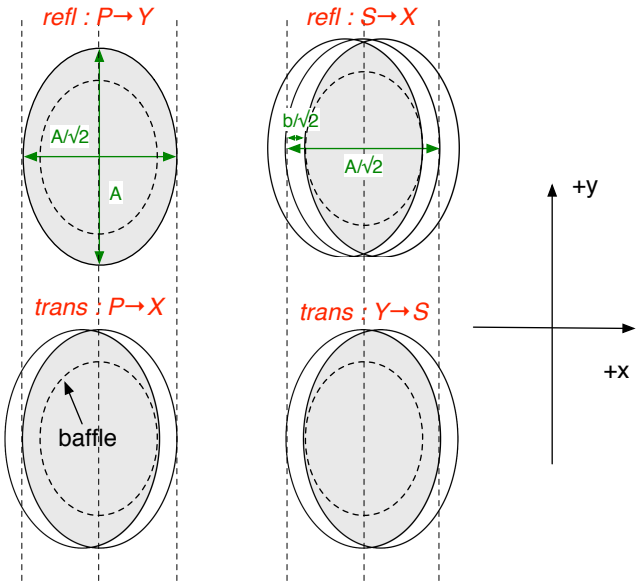

Figure 2 Clear aperture
Gray areas show clear apertures and the dash oval shows the size of baffle.

In Fig. 2, gray areas show clear apertures for the two reflections and two transmissions going from side1 to side2. The dash oval shape shows the BS baffle with a size of 21cm x 26cm aperture.

Maps of reflections from PRC to Y arm (SRC to X arm) is referred as RPY (RSX) and maps of transmission from PRC to X arm (SRC to Y arm) is referred to as TPX (TSY).

3. Maps

Fig.3 and 4 show the maps using the data in E1000788. Only tilt components are removed by using a field normal incident to the BS.

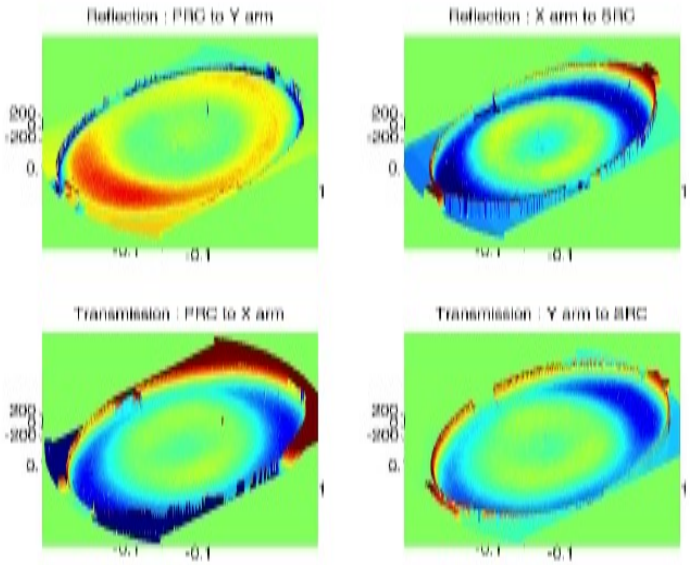

Figure 3 3D view of transmission and reflection maps

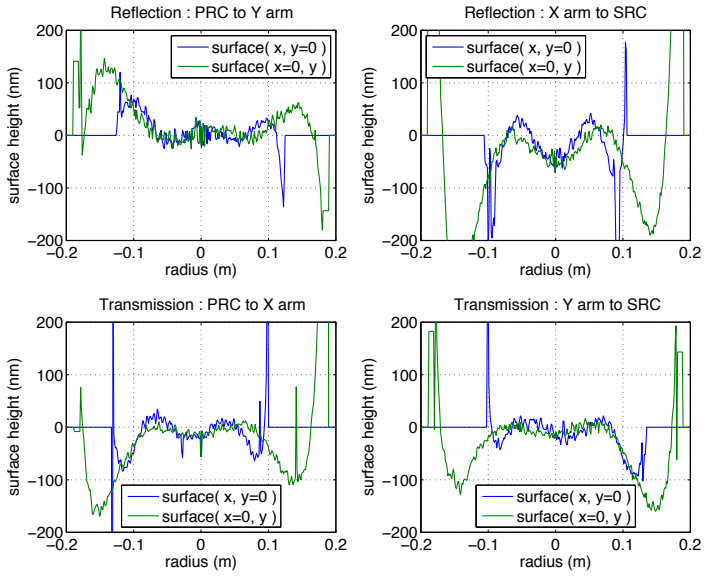

Figure 4 Cross sections of the map

4. 45° vs normal incident measurements

Another measurement done for the BS02 is the reflection map using a normal incident beam to the HR side of BS02. This map is compared with the reflection map PRC to Y arm by scaling the magnitude by √2 and shrinking the x coordinate by √2.

$$BSnorm(x,y) = \sqrt{2}\ data(\sqrt{2}x, y)$$

When the normal incident data are referred, it refers to BSnorm defined in this equation.

Fig.5 shows the comparison of maps of the reflection from PRC to Y arm with 45° incident beam and the reflection using normal incident beam, in the horizontal and vertical plane.

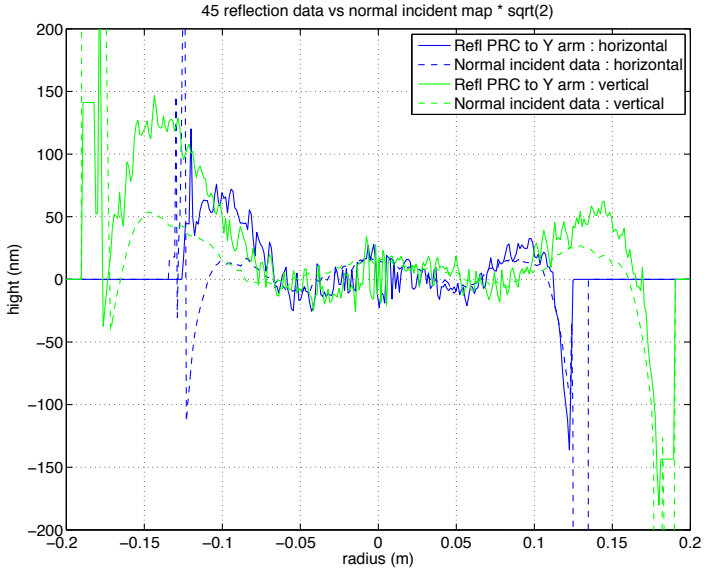

Figure 5. Reflection PRC to Y arm vs normal reflection

It is observed that the reflection measurement at 45°, solid lines, is noisier in the short wavelength region than the normal incident measurement, dashed lines. The figures in the central region are similar, but the magnitude of the RPY map is larger that the normal map outside of the central region.

In order to quantify this different, PSDs of the four maps with 45° incident angles and the normal incident data are compared in Fig.6. The 1D PSD used here is defined as follows:

$$PSD_{1D}(f) = \int_0^{2\pi} d\varphi_f PSD_{2D}(fx, fy)$$

As can be seen by comparing the solid blue line (45° reflection on the HR side, RPY) and the dashed blue line (normal incident data), the PSD of the RPY is higher than that of the normal map in the high frequency component.

All four maps measured using the 45° incident beam show similar behavior in the higher frequency region.

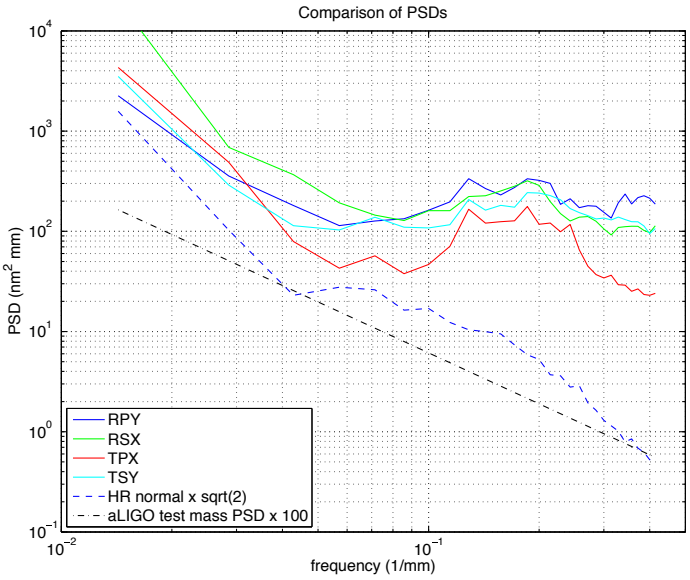

Figure 6. Comparison of PSDs.
Two 45° reflections (RPY solid blue, RSX) and transmissions (TPX, RSY) and the normal incident data (blue dashed). The dotted dashed line is 100x of aLIGO test mass PSD.

5. Mode analysis

In order to quantify the effects of these aberrations of the transmission and reflection maps, the loss of the TEM00 mode by these maps are calculated using the following coupling amplitude:

$$A_{mn} = \int dx\, dy TEM_{00} \cdot TEM^{*}_{mn} \cdot \exp(ik\delta(x,y)) \cdot baffle$$

where TEM is the mode shape on the BS, beam width of 5.3cm, δ is the reflection and transmission maps and the baffle is an oval with aperture size of 21x26cm.

The effect of the baffle is 140ppm, calculated by $1-|A_{00}(\delta=0)|^2$. As is shown later, this is negligible compared to effects of the BS map aberrations.

Four quantities were calculated

- 00 loss : $1 - |A_{00}|^2$
- lower order figures : $|A_{10}|^2+|A_{01}|^2+|A_{20}|^2+|A_{11}|^2+|A_{02}|^2$
- medium order modes : $\sum_{m+n\geq 3}^{m,n\leq 20} |A_{mn}|^2$
- higher order modes : 00 loss – lower order modes = $\sum_{m+n\geq 3} |A_{mn}|^2$

Table 1 shows these values for the map using normal reflection and four maps using 45° incident fields. Values are in units of 100ppm or 10^{-4}, and the loss by the baffle is 1.4 with this unit.

	normal	RPY	RSX	TPX	TSY
00 loss	20	56	220	58	57
Lower order figure	6.5	4.6	78	7.0	6.7
Medium order modes	10	19	120	34	28
Higher order modes	13	51	140	51	50

Table 1 Higher order modes induced by maps in units of 100ppm

Lower order figures for the normal case and RPY are almost the same, and the magnitude of the lower order figures in the four BS maps will be of that order, i.e., the astigmatism caused by the measurement setup will be small. Two transmissions, TPX and TSY, show similar values, but that for the reflection on the AR side, RSX, is order of magnitude larger. RSX includes disturbance by two paths through the BS, the reflection by the HR and the twice of AR. The power in the table is proportional to the square of the sum of these effects.

As is seen from Fig.6, high spatial frequency components measured using 45° beam can be mostly due to measurement noise. But the PSD of RSX shows that this map is dominated by low frequency components and medium order modes will not be affected much by the measurement errors.

Fig. 7 compares modes power, $|A_{ij}|^2$, induced by the map using the normal incident measurement, solid lines, and by the map of RPY, dashed lines. It is clear that the RPY map induces more higher order modes, which is consistent with the comparison of PDSs in Fig.6.

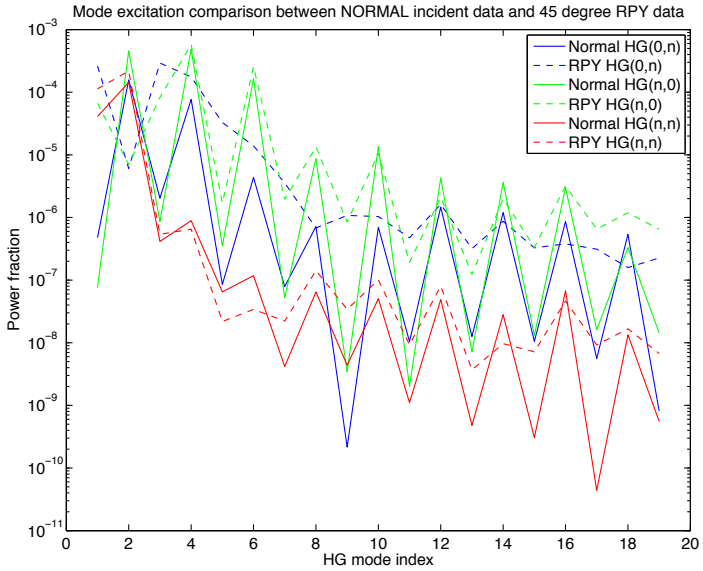

Figure 7 Power fraction of modes induced by the normal data map and RPY

Without extra measurements with reduces high frequency noises, the 00 mode loss cannot be estimated with higher accuracy, but the arguments above suggests that the loss by RSX is order of 1-1.5% in power, or 10% in amplitude.